

# Evolution and Statistics of the Geomagnetic Energy and Its Characteristic Timescales Since 1840



S. V. Starchenko and S. V. Yakovleva

**Abstract** The evolution of total (integrated from the core-mantle boundary to infinity) geomagnetic energy based on the COV-OBS.x1 geomagnetic field model is approximated by exponential functions with an error less than 3% in four time intervals between 1840 and 2020. Characteristic timescale is determined as a ratio of the energy to its time derivative ( $T = E/P$ , where  $P = dE/dt$  has a meaning of power). Timescale values are statistically explored with annual resolution. Most of the timescales (87%) are negative, indicating decrease of energy with characteristic times of the order of thousand years. The remaining 13% indicate the energy increase with the minor timescales of about a few thousand years. The median timescale is  $-1176$  years, the arithmetic mean is  $+1889$  years and the most probable or mode  $M_o = -483$  years. The large standard deviation and RMS (44,571 and 44,400 years) indicate heavy tails which are clearly seen in the bimodal probability density distribution. We define a special geometric mean timescale ( $-174$  years) which is consistent with the known convective velocities  $\sim 0.3$  mm/s and the observable magnetic heterogeneities drifts. The prevalent timescales are from  $\sim 500$  years to a few thousand years. Corresponding characteristic velocities or the mean field alpha effects ensure a subcritical geodynamo regime. The results are also consistent with periodical and spectral estimates from geodynamo simulations and geomagnetic field models for both the modern era and the ancient geomagnetic field. We estimate roughly that a comparable timescale for magnetic field is about a factor of two longer than  $T$ , while the magnetic field periodicity may be several times longer.

**Keywords** Geodynamo · Geomagnetic energy · Geomagnetic variations · Timescales

---

S. V. Starchenko (✉) · S. V. Yakovleva

Pushkov Institute of Terrestrial Magnetism, Ionosphere and Radio Wave Propagation, Russian Academy of Sciences (IZMIRAN), Kaluzhskoe hwy 4, Troitsk, Moscow 108840, Russia

## 1 Introduction

The observed variations of the main magnetic field generated in the Earth's core have characteristic timescales that exceed several years, since shorter variations are almost completely shielded by the electrically conductive mantle [1–4]. Exceptions, relatively small in terms of their energy, are short-term phenomena such as torsional oscillations [5–9] with periods of a few years and jerks with durations of about a year [10–13], subject of active current study.

Changes of the Earth's internally generated magnetic field spanning the time scales from a few years to a few thousand years are classified as secular variation (SV) [14, 15]. The main characteristic of SV is its period; however, strictly speaking, it is not a period, but rather a characteristic time or timescale, since SV periodicity in the mathematical sense of the word has not been proved. This variation results from the effect of magnetic induction in the fluid outer core and from effects of magnetic diffusion in the core and the mantle [16, 17].

Temporal spectrum of the observed geomagnetic field has a semi-discrete structure described by the following three types of variations [18–23].

1. Variations of the first type are characterized by harmonic periods from a few tens up to a hundred years (in particular  $T = 20, 30$  and  $60$  years). These variations are likely to be of internal origin, potentially being a manifestation of torsional oscillations in the fluid core [24]. The morphology of these variations and the high correlation with changes in the Earth's diurnal rotation also confirm their classification as torsional [25–28]. The physical nature of this class of variations as well as the mechanism of torsional waves generation is however still a matter of debate [5–9, 16, 29].
2. The main part of the SV spectrum includes periods of several hundred and several thousand years (in particular,  $360, 600, 900, 1200, 1800, 2700, 3600, 5400$  and  $9000 \pm 10\%$  years). These variations occur in the upper part of the core (or at the core-mantle boundary) due to thermal and compositional convection, propagation of magnetohydrodynamic waves and short-scale diffusion processes [17, 30–35]. The variation of  $9000 \pm 1000$  years is interpreted as the natural oscillation of the hydromagnetic dynamo [17, 19, 22, 32].
3. Fluctuations with timescales of tens of thousands of years and longer are primarily connected with decay modes, which are not oscillations. They result from magnetic diffusion processes in the entire core [14, 32–34]. Here we do not consider the longer variations, because they could hardly be covered by the model used in the present work, restricted by only  $< 200$  years of observations.

Determination of the geomagnetic field frequency/time characteristics has always been an important problem, which has been approached using various mathematical methods: spectral Fourier analysis [28, 36], maximum entropy method [37, 38], autoregressive and correlation methods [39], and wavelet analysis [40, 41]. A detailed review of mathematical approaches used in the search of periodicities in geomagnetic data series is presented in [42, 43] and references therein.

One of the most significant limitations of the above-mentioned essentially harmonic methods [38–43] is the fundamental impossibility of studying a period exceeding the length of the time series. For example, according to tests performed by Jackson and Mound [24], the longest meaningful period would not exceed 75% of the time series length. Besides, an assumption about broadband continuous spectrum of field variability becomes more and more popular [17, 42–45]. Already in 1983 Barton [46] performed spectral analysis of declination and inclination time series, concluding that there was no evidence for discrete periods but, instead, for bands of preferred periods at 60–70, 400–600, 1000–3000 and 5000–8000 years. Still earlier, in 1968, Currie [47] argued that the temporal power spectrum of geomagnetic field observations was governed by a power law, i.e.,  $f^k$ , where  $f$  is the frequency. More recently, Olson et al. [17] and Bouligand et al. [48, 49] carried out a detailed study of the frequency spectrum of dipole field variations from numerical geodynamo simulations, and found a broadband variability appropriately described by power laws. Their results agree well with the composite paleomagnetic dipole spectrum [50].

Against this background of numerous attempts of revealing any periodicity or characteristic times, we developed an original statistical approach to determining the long-term characteristics of time series [51–54]. For our studies, we chose the totally integrated energy  $E$  of the observed potential part of the main geomagnetic field [52–54]. This energy could be formally derived by means of the well-known work of Lowes [55], but apparently this was made only much later [56, 57]. This total energy seems to be the most adequate global variable for studying global temporal variations of the observed geomagnetic field.

The study of the energy contained in the potential part of the main geomagnetic field was initiated in [58]. Based on this work, Lowes [55, 59] determined the contribution of  $n$ -th spherical harmonic degree to the radial energy density normalized by the area of the sphere:

$$R_n = (n + 1) \left(\frac{a}{r}\right)^{2n+4} \sum_m^n [(g_n^m)^2 + (h_n^m)^2] \tag{1}$$

Here  $g_n^m$  and  $h_n^m$  are standard Gauss coefficients,  $a$  is the radius of the Earth and  $r$  is the radius of a sphere that varies from the core radius  $r_c$  to infinity. The resulting  $R_n$  is expressed in (Tesla)<sup>2</sup>.

Expression (1) is the so-called “spatial Lowes-Mauersberger power spectrum”. We prefer (perhaps, more physically correct) to name it  $r$ -density spectrum of energy renormalizing it to J/m. This density varies with  $r$ , while the total energy  $E$  is spatially independent, compare with [43]. To derive an expression for energy, we first obtain the contribution of the  $n$ -th harmonic degree  $R_n$  (in J/m) to the radial energy density of the potential field as

$$\frac{4\pi r^2}{2\mu_0} R_n = 2\pi a^2 \frac{n + 1}{\mu_0} \left(\frac{a}{r}\right)^{2(n+1)} \sum_{m=0}^n [(g_n^m)^2 + (h_n^m)^2] \tag{2}$$

Integrating (2) along the radius from the core-mantle boundary  $r = r_c$  (where  $r_c$  is the radius of the Earth's core) to infinity we obtain the contribution of the  $n$ -th harmonic degree to the total energy (in J) as:

$$\begin{aligned} E_n &= 2\pi a^{2n+4} \frac{n+1}{\mu_0} \sum_{m=0}^n [(g_n^m)^2 + (h_n^m)^2] \int_{r_c}^{+\infty} \frac{dr}{r^{2n+2}} \\ &= \frac{2\pi a^3}{\mu_0} \left(\frac{a}{r_c}\right)^{2n+1} \frac{n+1}{2n+1} \sum_{m=0}^n [(g_n^m)^2 + (h_n^m)^2] \end{aligned} \quad (3)$$

There is actually no need to integrate to infinity since even when integrating up to  $r$  equal to several times  $r_c$ , one obtains practically the same result with error less than 0.3%.

The integral energy  $E$  used in this study is simply the sum of all  $E_n$  terms from (3).

We use this  $E$  to obtain timescales  $T = E/(dE/dt)$  which will be defined in detail in the next section. As an analogue to our timescales we consider the instantaneous correlation time of Hulot and Le Mouél [60] involving the ratio of the Gauss coefficients to their time-derivatives as

$$\tau_n = \left\{ \frac{\sum_{m=0}^n [(g_n^m)^2 + (h_n^m)^2]}{\sum_{m=0}^n [(\dot{g}_n^m)^2 + (\dot{h}_n^m)^2]} \right\}^{1/2}. \quad (4)$$

This timescale is usually linked to spectrum (1) by many authors [33, 44, 48, 49] studying the geomagnetic field variation and  $\tau_n$  is one of the most popular characteristic timescale definitions. However, it is not so good for global investigations because it is a function of  $n$ . A more significant limitation of the correlation time (4) is that it is defined only on the Earth's surface. At the same time, the geomagnetic field energy is dominated by contributions from the regions located near the Earth's core, which is obvious from formulae (2) and (3). The integral energy  $E$  proposed here and all its derivatives are free from these disadvantages [52–54].

The primary goal of this paper is to explore global characteristic geomagnetic timescales. The detailed definition of these follows in Sect. 2 where we explore the 1840–2020 evolution of  $E$  and its timescales  $T$ . Section 3 deals with statistical and probability distribution descriptions of the annual energy timescales  $T$ . In Sect. 4 we outline the most statistically significant characteristic timescales for the geodynamo correlating them with modern/ancient geomagnetic field, trends, alpha effects, drifts and fluid velocities in the Earth's core. Final Sect. 5 presents a brief discussion and conclusions of this study.

## 2 Energy Evolution and Discrete Timescales

The central idea of this paper is to define and explore the characteristic instantaneous geomagnetic timescales  $T$  as the ratio of the global energy  $E$ , as defined by formula (3), to its time-derivative, referred to thereafter as power  $P = dE/dt$ . Thus, by definition

$$T \equiv E/(dE/dt) \quad (5)$$

An immediate bonus of this definition is introducing a positive/negative sign of the timescale  $T$ . The sign indicates rise/decay of the energy  $E$ . Definitions similar to (5), but without taking sign into account and in most cases local, has long been used [22, 33, 49, 60–62]. The innovation of our study is however to apply timescale definition (5) to a global evolutionary and statistical analysis of geomagnetic energy as defined by (3).

The simplest time-process related to definition (5) is the one with  $T = \text{const}$ . Viewing (5) as a differential equation, we introduce its solution as an exponential dependence:

$$E = C \exp(t/T) \quad (6)$$

Therefore, a reasonable initial step would be to model the evolution of  $E$  by exponents (6) on some suitable time intervals where the timescale  $T$  could be regarded as constant.

We use the open-source (<http://www.spacecenter.dk/files/magnetic-models/COV-OBSx1>) geomagnetic model COV-OBS.x1 [63, 64]. It spans 1840–2020 and is based on annual initial data. The authors of the model successfully extrapolated it down to the half-year ( $\text{yr}/2$ ) resolution. We used the results of this extrapolation for definition of the annual time-derivative  $dE/dt$ . It was calculated for each year as a ratio  $[E(t - \text{yr}/2) - E(t + \text{yr}/2)]/\text{yr}$ . Here  $t$  is the particular year and  $\text{yr}$  is 1 year. The corresponding time-values are transformed into seconds for calculating  $P = dE/dt$  in Watts.

Figure 1 shows the evolution of the energy  $E$  and power  $P = dE/dt$ . At two instances, marked in Fig. 1, the power becomes zero, which corresponds to the local energy extrema. These naturally divide the plot of  $E$  into three monotonous parts that can be approximated by exponential functions (6) with an error less than 2% for two intervals from 1932 to 2020, whereas the first interval 1840–1931.5 was approximated with error about 5%. Dividing this interval into two, we reduce the approximation errors to their minimum values placing the dividing point near the first local maximum of  $P$ . We consider important to have an error sufficiently lower than the energy variation  $2(E_{\max} - E_{\min})/(E_{\max} + E_{\min}) = 0.07$ . Thus, we split the evolution of  $E$  for the given time interval into 4 epochs approximated with an error  $\delta$  less than 3% ( $t$  is the time in years) as:

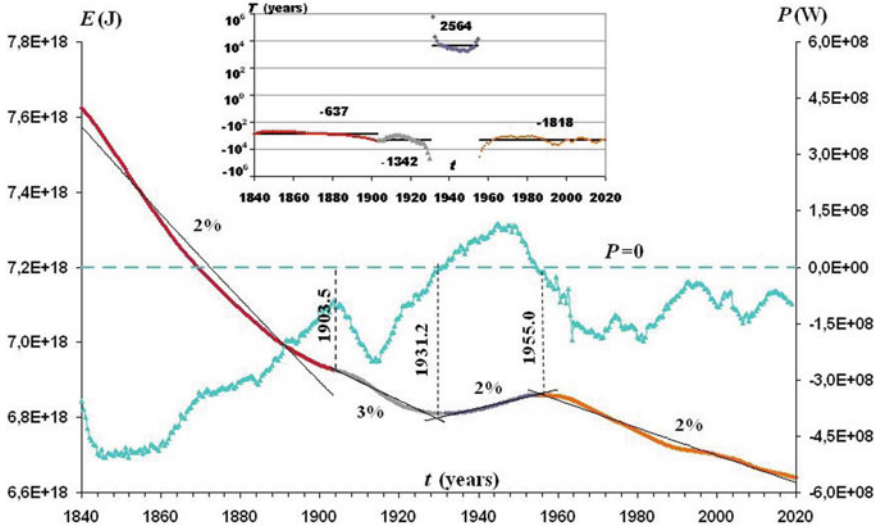


**Fig. 1** Evolution of the global energy  $E$  (multicolor) and power  $P$  (blue) obtained from COV-OBS.x1 model [63, 64]. The left vertical axis is for  $E$  (Joules), the right for  $P$  (Watts). Exponential functions (7) approximate the energy  $E$  with approximation errors  $\delta$ , indicated as a percentage. The horizontal dashed line corresponds to  $P = 0$ . The inset shows the continuous evolution of timescales  $T$  in years following (5). The relevant sections of the evolution of the energy and timescales are marked with the same colors. The corresponding discrete timescales (7–8) are displayed by horizontal lines

$$\left\{ \begin{array}{l} E = 136 \cdot e^{t/T_a} \cdot 10^{18} \text{ J, where } 1840 < t < 1903.5 \text{ and } \delta = 2\% \\ E = 28.6 \cdot e^{t/T_b} \cdot 10^{18} \text{ J, where } 1904 < t < 1931.5 \text{ and } \delta = 3\% \\ E = 3.22 \cdot e^{t/T_c} \cdot 10^{18} \text{ J, where } 1932 < t < 1955.5 \text{ and } \delta = 2\% \\ E = 19.9 \cdot e^{t/T_d} \cdot 10^{18} \text{ J, where } 1956 < t < 2020 \text{ and } \delta = 2\% \end{array} \right. \quad (7)$$

At this level of accuracy those exponential functions are indistinguishable from linear fits. However, we can still extract timescales with errors of the order a few percents in a sense of (5–6). Accordingly, the ratio of energy to power ( $T = E/P$ ) gives preliminary and rather rough discrete (in spectral sense) timescales for these four epochs (7) in years:

$$T_a = -637; T_b = -1342; T_c = 2564; T_d = -1818. \quad (8)$$

Now, we apply (5) and calculate the continuous evolution of the timescales for every year from 1840 to 2020. The result is shown in the inset to Fig. 1. The evolution is divided into relatively long, up to several decades, epochs alternating with short hyperbolic  $T$ -transitions. Hyperbolic  $T$ -transitions can have duration of several years and associated with the extrema of the energy where  $P = 0$  and  $|T|$  tends to infinity.

### 3 Statistics of the Characteristic Timescales

Following Fig. 1, we can reasonably split the energy evolution during 1840–2020 into four statistically different intervals (7). Each interval is described with a single spectral line or constant timescale  $T$ , (Eq. (8) and Fig. 1). The longest intervals are characterized with negative timescales indicating energy decrease. We observe three intervals with negative  $T$  and only one interval with positive  $T$ .

The intervals with negative  $T$  allow to estimate roughly the most probable ( $- 637$  years) and median (about  $- 1500$  years) timescales. At the same time, the shortest interval with positive timescales (2564 years) corresponds to a minor mode in a bimodal timescale distribution.

We now explore statistical and spectral features of annual timescales.

We apply formulae (5) and (3) to the Gauss coefficients provided by the COV-OBS.x1 model [64], and calculate 180 annual  $T$  values. The obtained timescales are then arranged in increasing order. This is essential for identifying extreme and median values, and for plotting probability distributions of  $T$ . The latter will be thereafter referred to as  $T_i$ , with  $i$  running from 1 to the maximum value  $I = 180$ .

Supposing that each  $T_i$  appears with the same probability, we plot the cumulative distribution function (thereafter CDF) for them as shown in Fig. 2.

The statistical parameters of the timescales are presented in a Table 1. All parameters were calculated from their standard definitions [65, 66] except for geometric mean (GM), which is explained at the end of this section.

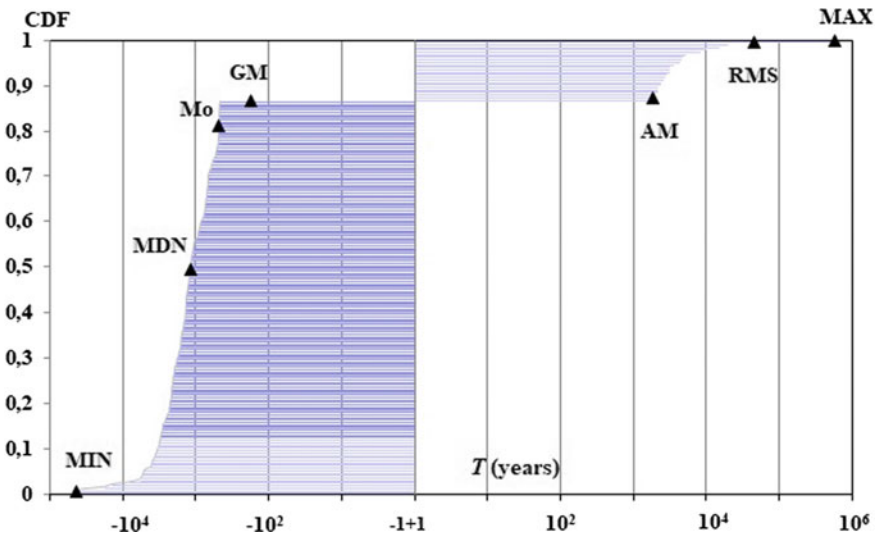


Fig. 2 The cumulative distribution function CDF for timescales  $T_i$  as defined in Sect. 2. Main statistical parameters of the timescales are shown (see Table 1 for details) with triangles. A confidence interval (75%) centered at MDN is shown in a darker color

**Table 1** Statistical parameters of the characteristic timescales  $T_i$ , years

Range of $T_i$	Number (i)	Minimum (MIN), median (MDN), maximum (MAX)			Arithmetic Mean (AM), Root Mean Square (RMS), Standard Deviation (SD), Geometric Mean (GM)			
		MIN	MDN	MAX	AM	RMS	SD	GM
All	180	-43,790	-1176	592,198	1889	44,364	44,571	-174
$T_i > 0$	24	1855	3127	592,198	29,309	121,055	119,980	4571
$T_i < 0$	156	-43,790	-1347	-464.8	-2329	5393	4880	-1380

We start our analysis from the general (calculated from all  $T_i$ ) median timescale  $MDN = -1176$  years (the first row of MDN column in Table 1). From this MDN we obtain a 75% confidence interval (based on the number of samples) bounded by timescales  $-3400$  and  $-470$  years that is visualized in Fig. 3. Therefore, the dominant trend is the decrease of energy with millennial characteristic timescales. This is similar to the timescales of drifts of the largest magnetic heterogeneities, and of the observed global geomagnetic variations [14, 35, 44, 61, 62, 67–70].

These 156 (87% of all  $T_i$ )  $T_i$  values with decreasing ( $T < 0$ ) energy may be viewed as reflecting a major timescale of the order of  $10^3$  years ( $-1347$  years in the MDN column, last line of the Table 1) characterizing the modern geodynamo with diminishing energy of the observed geomagnetic field. This is in agreement with the characteristic timescale for the dipolar component of the geomagnetic field [15, 17, 32, 35, 60, 61].

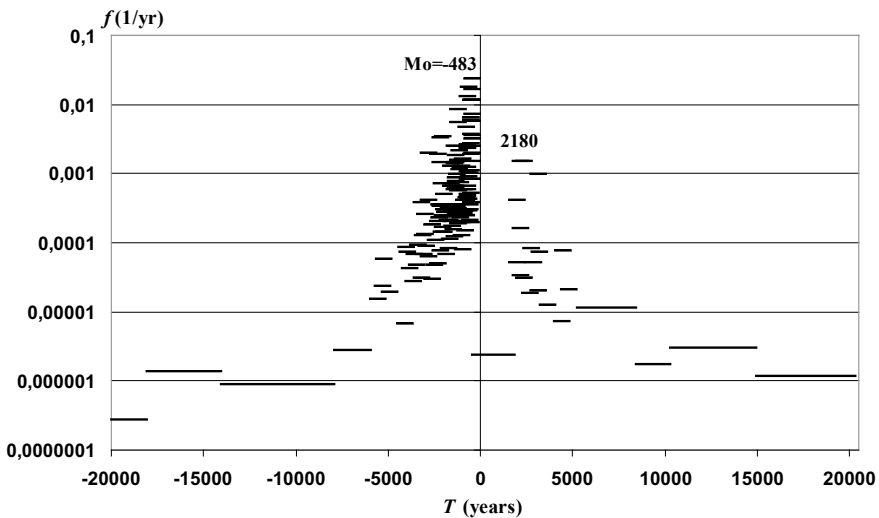


**Fig. 3** The probability density function  $f(T)$  as defined by formula (11). The most probable or mode value is  $M_0 = -483$  years and the secondary positive mode is 2180 years



The remaining 13% or 24 positive  $T_i$  values indicate the energy increase of a timescales of about a few thousand years (3127 years in MDN column, second line of Table 1).

General arithmetic mean AM is 1889 years (the first line in the AM column of Table 1). This positive value does not seem appropriate bearing in mind the domination of negative timescales. An explanation to this apparent contradiction is the large standard deviations and RMS values. Indeed, we observe heavy tails which are linked to extreme minimal ( $-43,800$  years) and maximal (592,000 years) timescales and are obviously overpopulated with respect to a Gaussian distribution. Thus, the true timescale distribution is not Gaussian but clearly bimodal. This is shown in Fig. 3 by a probability density function  $f(T)$ , which we defined as the simplest finite difference of CDF (see Fig. 2)

$$f_k = (I - 1)^{-1}(T_{k+1} - T_k)^{-1}. \tag{9}$$

Here a density function  $f(T) = d\text{CDF}/dT$  is a constant  $f_k$  for  $T_{k+1} < T < T_k$ , and  $k$  runs from 1 to  $I - 1$ . Outside the  $[T_1, T_I]$  interval  $f(T) = 0$ . The integral of  $f dT$  over all  $T$  is obviously equal to one. The most probable, or mode, value  $Mo$  would then be  $-483$  years. It is respectively two and four times smaller than the median and mean values considered above. Besides, we observe extremely uneven  $f$  variation and very large range of timescales covering more than 9 orders of magnitude from a value lower than  $-10^4$  years up to over than  $10^5$  years.

In view of the above, a geometric mean should be a more appropriate measure of a characteristic mean timescale. The geometric mean is well-defined for positive-only values (see GM column in the Table 1 for  $T_i > 0$ ), and can similarly be defined for  $T_i < 0$  as follows:

$$GM_+ = \left( \prod_{i=157}^{180} T_i \right)^{1/24} = 4571 \text{ years}, \quad GM_- = - \left( \prod_{i=1}^{156} |T_i| \right)^{1/156} = -1380 \text{ years} \tag{10}$$

Introducing  $S = \sum \text{sgn}(T_i) \lg |T_i|$  we write  $GM_{\pm} = \text{sgn}(S)10^{|S|/L}$ , where  $L$  is 24 for positive and 156 for negative  $T_i$ . Combining these expressions for positive and negative  $T_i$ , we obtain for a general geometric mean (note the minus sign in the exponent to  $GM_+$ ):

$$GM = -|GM_-|^{156/180}(GM_+)^{-24/180} = -174 \text{ years} \tag{11}$$

This value reflects a characteristic “rapid” change of the energy  $E$  in the modern era. Besides,  $|GM|$  is close to the length (180 years) of the field annual means series. The corresponding geomagnetic field timescale is about  $2GM = -348$  years, doubled due to the proportionality of the energy to the square of the field.

Let us round up this section by pointing out that there exists an extended gap containing no  $T_i$ 's (Fig. 2). The range of missing values extends from the maximum

negative  $T$  value (column MAX in Table 1) of  $-465$  years to the minimum positive  $T$  value (column MIN) of  $+1855$  years. A timescale within this gap might occur, but with very low probability, as seen in Fig. 3.

## 4 Physical Interpretation of Timescales Statistics

In order to make physical interpretation we need to compare our magnetic energy timescales (5) with known timescales of the magnetic field. Generally, such a comparison could be done by magnitude only, because there are rather different definitions of the timescales, e.g., compare expression (4) from Hulot and Le Mou el [60] with our expression (5) based on (3). Taking into consideration that axial dipole component is dominant everywhere, we could establish a rough relationship between our timescales  $T_0$  and  $\tau_0$ , similar to Hulot and Le Mou el's definition:

$$T_0 = |(g_1^0)^2/[d(g_1^0)^2/dt]| = |g_1^0/[dg_1^0/dt]|/2 = \tau_0/2. \quad (12)$$

We thus assume that our energy timescale is roughly a half of magnetic field timescale defined in a way similar to our definitions (3) and (5). This also follows from the simple consideration that the energy  $E$  is proportional to a square of the magnetic field intensity. Carrying out a Fourier transform on both parts of this relationship one sees immediately that an energy frequency is twice the magnetic field frequency.

An absolute value of the median energy timescale  $|\text{MDN}| = 1176$  years corresponds to a geomagnetic field timescale of 2352 years. This is about 30% larger than the exponential decay time of the modern axial dipole, which is about 1700–1900 years and characterized by decreasing trend [32, 34, 35, 71]. Therefore, the magnetic field associated with energy  $E$  apparently decays slower even in comparison with the slowest decay mode of the axial dipole.

Dividing the radius of the Earth's core ( $r_c = 3.5 \times 10^6$  m) by this characteristic time (2352 years), we obtain  $\alpha = 0.04$  mm/s, which is an order of magnitude less than the known convective velocities [14, 35, 67, 72–77]. Therefore,  $\alpha$  should roughly be an analogue of the alpha effect of the mean field theory [77–81]. However, it works against generation reducing the magnetic field intensity because all timescales  $\text{MDN} < 0$ . To consider the generation we use positive timescales ( $\sim 4000$  years, the second row of MDN/GM column in Table 1) giving  $\alpha_+ = 0.02$  mm/s. The known molecular magnetic diffusion is about  $1 \text{ m}^2/\text{s}$  [80], while the plausible turbulent mean field diffusion  $\eta$  could be a few times larger [77–81]. Thus, a mean-field magnetic Reynolds number value  $\text{Rm}$  is:

$$\text{Rm} = \alpha_+ r_c / \eta \approx 20 - 40. \quad (13)$$

This value is subcritical for a mean-field geodynamo [81–83]. The integral energy  $E$  decays due to prevalence of negative timescales over the positive, as shown above.

Let us find a correlation between the theoretically known [14, 35, 67, 72–77] convective velocities and corresponding observational drift velocities of magnetic heterogeneities [14, 35, 44, 61, 62, 67–70]. The convective velocities and drift velocities in the Earth’s core are of the order of 0.3 mm/s. Dividing the radius of the Earth’s core by these velocities, we obtain the values  $\sim 350$  years that are approximately twice the absolute value of the geometric mean timescale  $|GMI|$ .

This 348 years global magnetic field timescale is comparable with global “single time constant of secular variation”  $\tau_{\text{sec}} = 535$  years defined by Christensen and Tilgner [33], who used a set of numerical dynamo models together with direct observations to derive scaling relations for magnetic energy. A similar value  $\omega^{-1} = 415$  years was obtained by Bouligand et al. [49] where in their abstract they say: “based on dynamo simulations, the authors argue that a prior for the observational geomagnetic field over decennial to millennial periods can be constructed from the statistics of the field during the short satellite era”. Adopting similar approach, we use bicentennial statistics to describe timescales from a half-thousand up to a half-million years.

## 5 Concluding Remarks

The central idea of this paper is to explore a characteristic timescale  $T$  which is defined as a ratio of the total geomagnetic energy  $E$  to its time derivative, or power  $P = dE/dt$ . The energy is defined as resulting from integrating from the core-mantle boundary to infinity. The major bonus of such definition is a possibility to determine from direct observation a number of timescales sufficiently larger than the length of the studied time series.

Thus, we can explore insufficiently studied millennia-long processes on the base of relatively short, but much better studied and detailed, time series covering less than several centuries. This is especially important for the geomagnetic variations of long, i.e., from 450 years for  $T$  in this study, and even much longer, up to half-million years, characteristic times, which could be obtained from rather short periods of direct measurements.

A novel feature we introduce is to consider the sign which appears at these timescales. Negative timescales  $T < 0$  correspond to energy  $E$  decrease, while positive ones to energy  $E$  rise. The definitions of timescales similar to our have long been used [22, 33, 49, 60–62], but these studies did not take a sign into the account.

We investigated evolution of the power  $P$  and 180 annual timescales obtained from COV-OBS.x1 model [63, 64]. The evolution of timescales  $T$  is naturally divided into relatively long, up to several decades, epochs with almost constant  $T$  alternating with short hyperbolic  $T$ -transitions. Hyperbolic  $T$ -transitions can have duration of several years and are associated with the extrema of the energy where  $P = 0$  and  $|T|$  increases infinitely.

For the study period covering 1840–2020, evolution of energy  $E$  is approximated by exponents with an error of less than 3% if the period is divided into four intervals.

Each interval is described with a single spectral line or constant timescale  $T$ . We observe three intervals with negative  $T$  and only one interval with positive  $T$ . The intervals with negative  $T$  allow to estimate roughly the most probable ( $-637$  years) and median (about  $-1500$  years) timescales. At the same time, the shortest interval with positive timescales ( $2564$  years) corresponds to the minor mode in a timescale bimodal distribution.

Statistical analysis of the annual  $T$  values determines their standard statistical characteristics.  $87\%$  of  $T$  values are negative and indicate the decreasing  $T < 0$  trend in energy with the major timescale in the order of one thousand years attributable to modern geodynamo. The remaining  $13\%$  indicate the energy increase on the minor timescale that is about a few thousand years. The median timescale is  $-1180$  years, while the arithmetic mean is  $+1890$  years. Less probable heavy tails associated with the extreme minimal ( $-43,800$  years) and maximal ( $592,000$  years) timescales are the likely reason for extremely large standard deviation and RMS values of  $44,400$  and  $44,600$  years respectively. There is a gap between  $-465$  and  $1855$  years with no  $T$ . However, any  $T$  could appear there with a probability similar to the probability for the revealed heavy tails.

We calculated and plotted the bimodal probability density function with the most probable value, or mode  $Mo \approx -500$  years. The absolute value of  $|Mo|$  is two-four times smaller than absolute values of median and mean considered above. The minor mode is about  $2000$  years. Additionally, we observe extremely non-smooth variations in this function and a very wide range of time scales, covering more than 9 orders of magnitude, from below  $-10^4$  years to more than  $10^5$  years.

A geometric mean appears a more suitable measure to represent averaged timescales. The mean geometric timescale,  $GM = -174$  years (Sect. 3), is consistent with the known convective velocities  $\sim 0.3$  mm/s, the observable magnetic heterogeneities drifts [14, 35, 68–70] and with global geomagnetic timescales of about  $500$  years found previously [33, 49].

The prevalent timescales are from half a thousand years, where the maximum number of timescales is concentrated, and up to a few thousand years. Corresponding characteristic velocities or the mean field alpha effects ensure subcritical geodynamo. The obtained results are also consistent with periodical and spectral estimates from geodynamo simulations and geomagnetic field models for both the modern era and the ancient geomagnetic field.

To conclude, we consider how timescales  $T$  introduced here relate to long-term periods  $Q$ , obtained from studies of geomagnetic field spectrum in paleomagnetic and geodynamo models. Timescales  $T$  as defined here have physical meaning only on the interval where the change in energy  $E$  is monotonous. For the geomagnetic field, this interval is approximately  $2T$  as follows from formula (12). A periodic process can then be subdivided into a minimum of two such intervals, one corresponding to increasing energy (field strength), and another to decreasing. Thus, in this case  $Q = 4T$ , but a large gap in the energy derivative  $dE/dt$  arises when energy evolution changes from growth to decrease. This gap can be made smaller if the period  $Q$  is subdivided into four intervals, approximately corresponding to a sinusoidal dependence monotonously growing from zero to a maximum, decreasing to zero and then

to a minimum, and finally growing back to zero, resulting in  $Q = 8T$ . Discontinuities can be further reduced by an approximation like one discussed in Sect. 2, Fig. 1 and formulae (7) and (8). This is of course only a rough estimate, and in order to reveal a relationship between  $Q$  and  $T$ , it would be necessary to compare the behavior of the same data series within the framework of the classical and our statistical spectral approach. However, for now, we restrict ourselves to the simplest relation

$$Q = AT \quad (14)$$

We assume an approximate value of  $A \approx 6$ , as an average resulting from the above estimates for  $Q$ . Bearing in mind a high uncertainty of this number, it can still be argued that the results of all long-term (covering  $> 10^4$  years) studies of geomagnetic field evolution known to us [23, 43, 48, 49, 84–87] agree reasonably well with the results obtained in this work based only on a 200-year long series.

**Acknowledgements** We would like to express our deep gratitude to two anonymous reviewers for their important and useful comments that helped us significantly revise and improve the manuscript.

## References

1. McDonald, K.L.: Penetration of the geomagnetic secular field through a mantle with variable conductivity. *J. Geophys. Res.* **62**, 117–141 (1957)
2. Braginsky, S.I., Fishman, V.M.: Magnetic field shielding in the mantle at conductivity concentrated near the boundary with the core. *Geomagn. Aeron.* **17**(5), 907–915 (1977)
3. Benton, E.R., Whaler, K.A.: Rapid diffusion of the poloidal geomagnetic field through the weakly conducting mantle: a perturbation solution. *Geophys. J. R. Astr. Soc.* **75**, 77–100 (1983)
4. Jault, D.: Illuminating the electrical conductivity of the lowermost mantle from below. *Geophys. J. Int.* **202**(1), 482–496 (2015)
5. Braginsky, S.I.: Torsional magnetohydrodynamic vibrations in the Earth’s core and variations in day length. *Geomagn. Aeron.* **10**, 1–8 (1970)
6. Maffei, S., Jackson, A.: Propagation and reflection of diffusionless torsional waves in a sphere. *Geophys. J. Int.* **204**(3), 1477–1489 (2016)
7. Gillet, N., Jault, D., Canet, E., Fournier, A.: Fast torsional waves and strong magnetic field within the Earth’s core. *Nature* **465**, 74–77 (2010)
8. Teed, R.J., Jones, C.A., Tobias, S.M.: Torsional waves driven by convection and jets in Earth’s liquid core. *Geophys. J. Int.* **216**(1), 123–129 (2019)
9. Gillet, N., Jault, D., Canet, E.: Excitation of travelling torsional normal modes in an Earth’s core model. *Geophys. J. Int.* **210**(3), 1503–1516 (2017)
10. Bloxham, J., Zatman, S., Dumberry, M.: The origin of geomagnetic jerks. *Nature* **420**, 65–68 (2002)
11. Mandea, M., Olsen, N.: Geomagnetic and archeomagnetic jerks: where do we stand? *EOS Trans. Am. Geophys. Union* **90**(24), 208–208 (2009)
12. Aubert, J., Finlay, C.C.: Geomagnetic jerks and rapid hydromagnetic waves focusing at Earth’s core surface. *Nat. Geosci.* **12**(5), 393–398 (2019)
13. Kloss, C., Finlay, C.C.: Time-dependent low-latitude core flow and geomagnetic field acceleration pulses. *Geophys. J. Int.* **217**(1), 140–168 (2019)
14. Parkinson, W.D.: *Introduction to Geomagnetism*. Scottish Academic Press, Edinburgh (1983)

15. Bloxham, J., Gubbins, D., Jackson, A.: Geomagnetic secular variation. *Phil. Trans. R. Soc. Lond. A* **329**, 415–502 (1989)
16. Wardinski, I.: Geomagnetic secular variation. In: Gubbins, D., Herrero-Bervera, E. (eds.) *Encyclopedia of Geomagnetism and Paleomagnetism*. Springer, Dordrecht (2007)
17. Olson, P., Christensen, U., Driscoll, P.: From superchrons to secular variation: a broadband dynamo frequency spectrum for the geomagnetic dipole. *Earth Planet. Sci. Lett.* **319–320**, 75–82 (2012)
18. Pecherskij, D.M., Sokolov, D.D.: *Paleomagnetology, Petromagnetology and Geology. Dictionary-reference for neighbors in the specialty*. IFZ RAS, Moscow (2010). <http://paleomag.ifz.ru> (in Russian)
19. Braginsky, S.I.: On the spectrum of oscillations of the earth hydromagnetic dynamo. *Geomagn. Aeron.* **10**(2), 221–233 (1970)
20. Braginsky, S.I.: Origin of the Earth's magnetic field and its secular variations. *Izvestiya Acad. Sci. USSR Phys. Solid Earth* **10**, 3–14 (1972)
21. Burlatskaya, S.P.: *Archaeomagnetism. The Structure and Evolution of the Earth's Magnetic Field*. GEOS, Moscow (2007) (in Russian)
22. Nachasova, I.E., Pilipenko, O.V.: *Archaeomagnetic studies at Schmidt institute of physics of the earth, Russian academy of sciences: history and main results*. *Izv. Phys. Solid Earth* **55**(2), 298–310 (2019)
23. Petrova, G.N., Nechaeva, T.B., Pospelova, G.A.: *Characteristic Variations in the Past Geomagnetic Field*. Nauka, Moscow (1992). (in Russian)
24. Jackson, L.P., Mound, J.E.: Geomagnetic variation on decadal time scales: what can we learn from empirical mode decomposition? *Geophys. Res. Lett.* **37**(14), L14307 (2010)
25. Braginsky, S.I.: Short-period geomagnetic secular variation. *Geophys. Astrophys. Fluid Dyn.* **30**(1–2), 1–78 (1984)
26. Bondar, T.N., Golovkov, V.P., Yakovleva, S.V.: Secular variation in the geomagnetic field in 1980–2000. *Geomagn. Aeron.* **43**(6), 799–802 (2003)
27. Ivanov, V.V., Bondar, T.N.: Dynamics and physical model of secular variations within a range of up to 100 years. *Geomagn. Aeron.* **55**(3), 389–397 (2015)
28. Allredge, L.R.: Geomagnetic variations with periods from 13 to 30 years. *J. Geomagn. Geoelectr.* **29**, 123–135 (1977)
29. Hulot, G., Finlay, C.C., Constable, C.G., Olsen, N., Mandea, M.: The magnetic field of planet Earth. *Space Sci. Rev.* **152**, 159–222 (2010)
30. Braginsky, S.I.: Magnetic waves in the core of the Earth. II *Geophys. Astrophys. Fluid Dyn.* **14**, 189–208 (1980)
31. Braginsky, S.I.: MAC-oscillations of the hidden ocean of the core. *J. Geomagn. Geoelectr.* **45**(11–12), 1517–1538 (1993)
32. Olson, H., Amit, Y.: Changes in Earth's dipole. *Naturwissenschaften* **93**, 519–542 (2006)
33. Christensen, U.R., Tilgner, A.: Power requirement of the geodynamo from ohmic losses in numerical and laboratory dynamos. *Nature* **429**, 169–171 (2004)
34. Starchenko, S.V.: Harmonic sources of the main geomagnetic field in the Earth's core. *Geomagn. Aeron.* **51**(3), 409–414 (2011)
35. Starchenko, S.V., Ivanov, V.V.: Nature of the diffusion, generation, and drift of the geomagnetic dipole from 1900 to 2010. *Dokl. Earth Sci.* **448**(1), 67–69 (2013)
36. Creer, K.M., Thouveny, N., Blunk, I.: Climatic and geomagnetic influences on the Lac du Bouchet palaeomagnetic SV record through the last 110 000 years. *Phys. Earth Planet. Inter.* **64**(2–4), 314–341 (1990)
37. Currie, R.G.: Geomagnetic line spectra – 2 to 70 years. *Astrophys. Space Sci.* **21**, 425–438 (1973)
38. Papitashvili, N.Y., Rotanova, N.M.: The method of maximum entropy and its application to the analysis of time series of the geomagnetic field. *Geomagn. Aeron.* **19**(3), 543–550 (1979)
39. Ivanov, V.V., Rotanova, N.M.: The Sompi spectral method and its application in the analysis of simulated and measured time series. *Geomagn. Aeron.* **36**(1), 89–94 (1996)

40. Burakov, K.S., Galyagin, D.K., Nachasova, I.E., Reshetnyak, M.Yu., Sokolov, D.D., Frick, P.G.: Wavelet analysis of geomagnetic field intensity for the past 4000 years. *Izv. Phys. Solid Earth* **34**(9), 773–778 (1998)
41. Rotanova, N.M., Bondar, T.N., Ivanov, V.V.: Wavelet analysis of secular geomagnetic variations. *Geomagn. Aeron.* **44**(2), 252–258 (2004)
42. Panovska, S., Finlay, C.C., Hirt, A.M.: Observed periodicities and the spectrum of field variations in Holocene magnetic records. *Earth Planet. Sci. Lett.* **379**, 88–94 (2013)
43. González-López, A., Campuzano, S.A., Molina-Cardina, A., Pavón-Carrasco, F.J., Osete, M.L.: Characteristic periods of the paleosecular variation of the Earth's magnetic field during the Holocene from global paleoreconstructions. *Phys. Earth Planet. Inter.* **312**, 106656 (2021)
44. Tanriverdi, V., Tilgner, A.: Global fluctuation in magnetohydrodynamics dynamos. *New J. Phys.* **13**, 033019 (2011)
45. Olson, P.: Core dynamics: an introduction and overview. In: *Treatise on Geophysics*, 2nd edn, vol. 8, pp. 1–25. Elsevier, Amsterdam (2015). <https://doi.org/10.1016/B978-0-444-53802-4.00137-8>
46. Barton, C.: Analysis of palaeomagnetic time series – technique and applications. *Geophys. Surv.* **5**, 335–368 (1983)
47. Currie, R.: Geomagnetic spectrum of internal origin and lower mantle conductivity. *J. Geophys. Res.* **73**, 2779–2790 (1968)
48. Bouligand, C., Hulot, G., Khokhlov, A., Glatzmaier, G.A.: Statistical palaeomagnetic field modelling and dynamo numerical simulation. *Geophys. J. Int.* **161**, 603–626 (2005)
49. Bouligand, C., Gillet, N., Jault, D., Schaeffer, N., Fournier, A., Aubert, J.: Frequency spectrum of the geomagnetic field harmonic coefficients from dynamo simulations. *Geophys. J. Int.* **207**, 1142–1157 (2016)
50. Constable, C., Johnson, C.: A paleomagnetic power spectrum. *Phys. Earth Planet. Inter.* **153**, 61–73 (2005)
51. Starchenko, S.V., Yakovleva, S.V.: MHD sources, 1600–2005 evolution and 1900–2005 probabilistic time analysis for logarithmic time-derivatives of geomagnetic spherical harmonics. In: Nurgaliev D., Shcherbakov V., Kosterov A., Spassov S. (eds) *Recent Advances in Rock Magnetism, Environmental Magnetism and Paleomagnetism*, pp. 513–522. Springer Geophysics. Springer, Cham. (2019)
52. Starchenko, S.V., Yakovleva, S.V.: Spatial-spectral evolution of the energy and power of the potential geomagnetic field since 1840. In: Bobrov, N.Yu., Zolotova, N.V., Kosterov, A.A., Yanovskaya, T.B. (eds.) *Proceedings of the Conference “Problems of the Geocosmos”*, 08–12 Oct 2018, Peterhof, St. Petersburg, pp. 236–243. VVM Publishing House, St. Petersburg (2018) (in Russian)
53. Starchenko, S.V., Yakovleva, S.V.: Determination of specific time variations in the energy of the Earth's magnetic potential field from the IGRF model. *Geomagn. Aeron.* **59**(5), 606–611 (2019)
54. Starchenko, S.V., Yakovleva, S.V.: Energy and power spectra of the potential geomagnetic field since 1840. *Geomagn. Aeron.* **59**(2), 242–248 (2019)
55. Lowes, F.J.: Mean-square values on sphere of spherical harmonic vector fields. *J. Geophys. Res.* **71**, 2179 (1966)
56. Xu, W.: Unusual behavior of the IGRF during the 1945–1955 period. *Earth Planets Space* **52**, 1227–1233 (2000)
57. Bayanjargal, G.: The total energy of geomagnetic field. *Geomech. Geophys. Geo-Energy Geo-Resour.* **1**(1–2), 29–33 (2015). <https://doi.org/10.1007/s40948-015-0006-y>
58. Mauersberger, P.: Das Mittel der Energiedichte des geomagnetischen Hauptfeldes an der Erdoberfläche und seine sakulare Aenderung. *Gerlands Beitr. Geophys.* **65**, 207–215 (1956)
59. Lowes, F.J.: Spatial power spectrum of the main geomagnetic field, and extrapolation to the core. *Geophys. J. R. Astr. Soc.* **36**, 717–730 (1974)
60. Hulot, G., Le Mouél, J.L.: A statistical approach to the Earth's main magnetic field. *Phys. Earth Planet. Inter.* **82**, 167–183 (1994)

61. Hulot, G., Sabaka, T.J., Olsen, N. Fournier, A.: The present and future geomagnetic field. In: *Treatise on Geophysics*, 2nd edn, vol. 5, pp. 33–78 (2015). <https://doi.org/10.1016/B978-0-444-53802-4.00096-8>
62. Lhuillier, F., Fournier, A., Hulot, G., Aubert, J.: The geomagnetic secular variation timescale in observations and numerical dynamo models. *Geophys. Res. Lett.* **38**, L09306 (2011)
63. Gillet, N., Jault, D., Finlay, C.C., Olsen, N.: Stochastic modeling of the Earth's magnetic field: inversion for covariances over the observatory era. *Geochem. Geophys. Geosyst.* **14**(4), 766–786 (2013)
64. Gillet, N., Barrois, O., Finlay, C.C.: Stochastic forecasting of the geomagnetic field from the COV-OBS.x1 geomagnetic field model, and candidate models for IGRF-12. *Earth Planet Space* **67**, 71 (2015)
65. Bowley, A.L.: *Elements of Statistics*, 336 pp. P.S. King, London (1902)
66. Freund, R.J., Mohr, D.L., Wilson, W.J.: *Statistical Methods*, 3d edn, 800 pp. Academic Press, Salt Lake City USA (2010)
67. Braginsky, S.I., Roberts, P.H.: Equations governing convection in the Earth's core and the geodynamo. *Geophys. Astrophys. Fluid Dyn.* **79**, 1–97 (1995)
68. Bullard, E.C., Freeman, C., Gellman, H., Nixon, J.: The westward drift of the Earth's magnetic field. *Philos. Trans. R. Soc. Lond. A* **243**(6), 1–92 (1950)
69. Yukutake, T.: The westward drift of the Earth's magnetic field in historic times. *J. Geomagn. Geoelectr.* **19**, 103–116 (1967)
70. Holme, R., Whaler, K.: Steady core flow in an azimuthally drifting reference frame. *Geophys. J. Int.* **145**, 560–569 (2001)
71. Poirier, J.P.: Physical properties of the Earth's core. *C. R. Acad. Sci. Paris, Sér. II* **318**, 341–350 (1994)
72. Aubert, J.: Approaching Earth's core conditions in high-resolution geodynamo simulations. *Geophys. J. Int.* **219**, 137–151 (2019)
73. Starchenko, S.V.: Analytic scaling laws in planetary dynamo models. *Geophys. Astrophys. Fluid Dyn.* **113**(1–2), 71–79 (2019)
74. Christensen, U.: Geodynamo models with a stable layer and heterogeneous heat flow at the top of the core. *Geophys. J. Int.* **215**, 1338–1351 (2018)
75. Starchenko, S.V., Jones, C.A.: Typical velocity and magnetic field strengths in planetary interiors. *Icarus* **157**, 426–435 (2002)
76. Busse, F.H.: Generation of planetary magnetism by convection. *Phys. Earth Planet. Inter.* **12**, 350–358 (1976)
77. Moffatt, K., Dormy, E.: *Self-Exiting Fluid Dynamos*. Cambridge University Press, Cambridge (2019)
78. Kleeorin, N., Rogachevskii, I.: Magnetic helicity tensor for an anisotropic turbulence. *Phys. Rev. E* **59**, 6724–6729 (1999)
79. Ruzmaikin, A.A., Starchenko, S.V.: Kinematic turbulent mean-field geodynamo. *Geomagn. Aeron.* **28**, 475–480 (1988)
80. Driscoll, P.E., Du, Z.: Geodynamo conductivity limits. *Geophys. Res. Lett.* **46**, 7982–7989 (2019)
81. Shukurov, A.M., Sokolov, D.D., Ruzmaikin, A.A.: Oscillatory  $\alpha^2$ -dynamo. *Magnetohydrodynamics* **21**(1), 6–10 (1985)
82. Starchenko, S.V.: Supercritical magnetoconvection in rapidly rotating planetary cores. *Phys. Earth Planet. Inter.* **117**(1–4), 225–235 (2000)
83. Starchenko, S.V.: Dynamo models with strong generation 1. Kinematic solution and axisymmetric  $\alpha\omega$ -dynamo. *Geophys. Astrophys. Fluid Dyn.* **77**, 55–77 (1994)
84. Bondar, T.N., Golovkov, V.P., Yakovleva, S.V.: Spatiotemporal model of the secular variations of the geomagnetic field in the time interval from 1500 through 2000. *Geomagn. Aeron.* **42**(6), 793–800 (2002)
85. Jackson, A., Jonkers, A.R.T., Walker, M.R.: Four centuries of geomagnetic secular variation from historical records. *Philos. Trans. R. Soc. Lond. A* **358**, 957–990 (2000)



86. Panovska, S., Constable, C.G., Korte, M.: Extending global continuous geomagnetic field reconstructions on timescales beyond human civilization. *Geochem. Geophys. Geosyst.* **19**(12), 4757–4772 (2018)
87. Morzfeld, M., Buffett, B.A.: A comprehensive model for the kyr and Myr timescales of Earth's axial magnetic dipole field. *Nonlinear Process. Geophys.* **26**(3), 123–142 (2019)